Syntheses, Crystal Structures and Optoelectronic Properties of Two New Inorganic Thioantimonates①

LI Ji-Long[a, b] MA Wen[b] JIN Jian-Ce[b]
FENG Mei-Ling[b②] HUANG Xiao-Ying[b]

[a] (*College of Chemistry and Materials Science, Fujian Normal University, Fuzhou* 350007, *China*)

[b] (*State Key Laboratory of Structural Chemistry, Fujian Institute of Research on the Structure of Matter, Chinese Academy of Sciences, Fuzhou* 350002, *China*)

ABSTRACT Two new thioantimonates, $(NH_4)_2Sb_{10}S_{16}$ (**1**) and $K_{1.4}(NH_4)_{0.6}Sb_{10}S_{16}$ (**2**), have been synthesized by solvothermal method with the yields of 80% and 85%, respectively. Single-crystal X-ray diffraction (SCXRD) study reveals that **1** crystallizes in the monoclinic space group of *Pn* with a = 8.1284(4), b = 19.4587(9), c = 9.1030(4) Å, β = 91.736(5)°, V = 1439.14(12) Å^3, Z = 2, D_c = 4.077 g·cm^{-3}, F(000) = 1576, μ = 10.389 mm^{-1}, R = 0.0343 and wR = 0.0624 ($I > 2\sigma(I)$); **2** also crystallizes in the monoclinic space group of *Pn* with a = 8.0989(6), b = 19.3730(17), c = 9.0411(6) Å, β = 91.879(6)°, V = 1417.79(19) Å^3, Z = 2, D_c = 4.207 g·cm^{-3}, F(000) = 1598, μ = 10.748 mm^{-1}, R = 0.0323 and wR = 0.0664 ($I > 2\sigma(I)$). The anionic frameworks of two compounds both feature two-dimensional (2*D*) $[Sb_{10}S_{16}]_n^{2n-}$ layers. The stabilities and optoelectronic properties of **1** and **2** have been characterized. In particular, they are stable under acidic or alkaline conditions (pH = 0 or 12.5), showing excellent acid-based resistance.

Keywords: solvothermal synthesis, crystal structure, thioantimonates, optoelectronic property;
DOI: 10.14102/j.cnki.0254–5861.2011–3075

1 INTRODUCTION

Metal sulfides have received widespread attention because of their fascinating structural diversities, and potential applications in catalysis[1, 2], ion exchange[3, 4], nonlinear optics[5], semiconductors[6], optoelectronics[7-9], *etc.*. Among them, thioantimonates(III) have been extensively studied due to the stereochemical effect of lone-pair electrons on Sb(III), by which Sb(III) can form various coordination geometries of $[SbS_m]$ (m = 3∼6), such as $[SbS_3]$[10], $[SbS_4]$[10], $[SbS_5]$[11] and $[SbS_6]$[12, 13]. These different structural units can be further polymerized to form a series of anionic polymeric moieties of $[Sb_xS_y]^{3x-2y}$ (*e.g.*, $[Sb_4S_7]_n^{2n-}$, $[Sb_5S_8]_n^{n-}$, $[Sb_5S_9]_n^{3n-}$, $[Sb_8S_{13}]_n^{2n-}$ and $[Sb_9S_{15}]_n^{2n-}$) with diverse dimensionalities by corner-sharing, edge-sharing, or face-sharing[14-21].

In recent decades, a large number of metal sulfides have been synthesized and prepared by high temperature solid state reactions[22, 23], molten salt reactions[24], reactions in deep eutectic solvents[25-27], solvothermal methods[13, 28-31], and so on. Among these synthetic methods, solvothermal methods have been proved to be very effective for the preparation of thioantimonates(III). Up to now, thioantimonates(III) with metal cations (*e.g.*, K^+, Cs^+, Ba^{2+}, Sr^{2+} and Tl^+)[11, 20, 32-34] or protonated organic amines (*e.g.*, $[Me_4N]^+$, $[Et_4N]^+$ and $[MeNH_3]^+$)[10, 13-19] as charge-balancing agents have been extensively reported, such as $(dienH_2)[Sb_8S_{13}]\cdot 1.5H_2O$[35], $(1,2\text{-dap}H)_2[Sb_8S_{13}]$[35], $(CH_3NH_3)_2Sb_8S_{13}$[18], $[C_8N_4H_{26}]_{0.5}[Sb_7S_{11}]$[36], $Cs_2Sb_4S_7$[37], $SrSb_4S_7\cdot 6H_2O$[33] and $BaSb_2S_4$[32].

It is also worthy to note that the anions $[Sb_5S_8]^{2-}$ or $[Sb_{10}S_{16}]^{2-}$ with the Sb:S ratio of 1:1.6 are particularly prevalent in thioantimonates(III) whose cations are usually protonated organic amines or inorganic ions, such as ASb_5S_8 (A = K, Tl)[11], $(C_3H_{12}N_2)[Sb_{10}S_{16}]$ ($[C_3H_{12}N_2]^{2+}$ = doubly protonated N,N-diethylethylenediamine)[38], $[C_6H_{17}N_3]Sb_{10}S_{16}$ ($[C_6H_{17}N_3]^{2+}$ = doubly protonated 2-piperazine-N-ethylamine

Received 21 December 2020; accepted 21 January 2021 (**CCDC 2051501 for 1 and 2051502 for 2**)

① This research was supported by the National Science Foundations of China (Nos. 22076185 and 21771183), the Natural Science Foundation of Fujian Province (No. 2020J06033) and FJIRSM&IUE Joint Research Fund (No. RHZX-2018-005)

② Corresponding author. E-mail: fml@fjirsm.ac.cn

cation)[18], $[H_3N(CH_2)_3NH_3]Sb_{10}S_{16}$ ($[H_3N(CH_2)_3NH_3]^{2+}$ = doubly protonated 1,3-propanediamine)[39], $[C_6H_{18}N_2]Sb_{10}S_{16}H_2O$ ($[C_6H_{18}N_2]^{2+}$ = doubly protonated 1,2-diaminopropane)[40]. However, it is rare for NH_4^+ to be introduced into thioantimonates(III) as charge-balancing agent to form the polymeric anions of $[Sb_xS_y]^{n-}$ except $NH_4Sb_4S_7$[41] and NH_4SbS_2[42]. Herein, we report two 2*D* thioantimonates(III) synthesized by the mild solvothermal reactions, namely $(NH_4)_2Sb_{10}S_{16}$ (**1**) and $K_{1.6}(NH_4)_{0.4}Sb_{10}S_{16}$ (**2**), which contain NH_4^+ and the mixed cations of NH_4^+ and K^+ as the charge-balancing agents, respectively. Their crystal structures, stabilities and optoelectronic properties were studied.

2 EXPERIMENTAL

All reagents and chemicals employed in this study were analytical reagents and commercially available without further purification. Single-crystal X-ray diffraction (SCXRD) data for **1** and **2** were collected by using graphite-monochromatized Mo-$K\alpha$ radiation (λ = 0.71073 Å) at 100 K on an Agilent Supernova Dual diffractometer with an Atlas detector. Elemental analyses (EA) of H, N and S were obtained by using a German Elementary Vario MICRO instrument. Solid-state ultraviolet-visible (UV-Vis) spectra were analyzed at room temperature with $BaSO_4$ as a standard (100% reflectance) using a Shimadzu UV-2600 spectrometer spectrophotometer. Powder X-ray diffraction (PXRD) measurement was performed at room temperature on a Miniflex II diffractometer at 30 kV, 15 mA using Cu$K\alpha$ radiation (λ = 1.54178 Å) in the angular range of 2θ = 5～50° or 5～55°. Thermogravimetric analyses (TGA) were performed with a NETZSCH STA449C thermogravimetric analyzer at a heating rate of 10 ℃·min^{-1} under a nitrogen atmosphere.

2. 1 Synthesis of $(NH_4)_2Sb_{10}S_{16}$ (1)

A mixture of $Sb(Ac)_3$ (0.5 mmol) and S (1.5 mmol) in a mixed solvent of 3 mL NH_3H_2O and 0.5 mL $N_2H_4H_2O$ was sealed in a 20 mL Teflon-lined stainless-steel reactor and heated at 180 ℃ for 5 days. Then the product was washed with distilled water and ethanol and then dried in air. The dark-red plate-like crystals of **1** were obtained with a high yield (71 mg, 80% based on $Sb(Ac)_3$). EA, calcd.: H, 0.46; N, 1.59; S, 29.04%. Found: H, 0.36; N, 1.64; S, 28.96%).

2. 2 Synthesis of $K_{1.4}(NH_4)_{0.6}Sb_{10}S_{16}$ (2)

A mixture of KCl (1.6 mmol), $Sb(Ac)_3$ (0.5 mmol) and S (1.5 mmol) in a mixed solvent of 2 mL NH_3H_2O and 1 mL $N_2H_4H_2O$ was sealed in a 20 mL Teflon-lined stainless-steel reactor and heated at 180 ℃ for 5 days. After that, the product was washed with distilled water and ethanol and then dried in air. The dark-red plate-like crystals of **2** were obtained with a high yield (77 mg, 85% based on $Sb(Ac)_3$). EA, calcd.: H, 0.13; N, 0.47; S, 28.56%. Found: H, < 0.3; N, 0.51; S, 28.76%).

2. 3 Structure refinements

The dark-red plate-like crystals **1** and **2** were selected for the diffraction experiment with dimensions of 0.20mm × 0.10mm × 0.02mm and 0.20mm × 0.05mm × 0.02mm, respectively. For **1**, a total of 11812 reflections were collected in the range of 3.331°≤θ≤31.200° with R_{int} = 0.0402, of which 6555 are independent. Crystal **1** crystallizes in the monoclinic *Pn* space group with: a = 8.1284(4), b = 19.4587(9), c = 9.1030(4) Å, β = 91.736(5)°, V = 1439.14(12) Å^3, Z = 2, D_c = 4.077 g·cm^{-3}, F(000) = 1576, μ = 10.389 mm^{-1}, R = 0.0343 and wR = 0.0624 ($I > 2\sigma(I)$). A total reflections of 9746 were collected in **2** in the range of 10.2°≤θ≤29.634° with R_{int} = 0.0376, 5225 of which are independent. Crystal **2** is also of monoclinic *Pn* space group with a = 8.0989(6), b = 19.3730(17), c = 9.0411(6) Å, β = 91.879(6)°, V = 1417.79(19) Å^3, Z = 2, D_c = 4.207 g·cm^{-3}, F(000) = 1598, μ = 10.748 mm^{-1}, R = 0.0323 and wR = 0.0664 ($I > 2\sigma(I)$). *SHELX* 2018 package was used to solve and refine the structure on F^2 by the full-matrix least-squares methods[43]. Selected bond lengths and bond angles of **1** and **2** are shown in Tables 1 and **2**, respectively, and selected hydrogen bonds are listed in Table 3.

Table 1. Selected Bond Lengths (Å) for 1 and 2

1		2	
Bond	Dist.	Bond	Dist.
Sb(1)−S(2)	2.454(3)	Sb(1)−S(2)	2.446(3)
Sb(1)−S(3)	2.486(3)	Sb(1)−S(3)	2.490(4)
Sb(1)−S(1)	2.546(3)	Sb(1)−S(1)	2.558(3)
Sb(2)−S(1)	2.443(3)	Sb(2)−S(1)	2.433(3)
Sb(2)−S(2)	2.656(3)	Sb(2)−S(2)	2.648(3)

To be continued

Sb(2)−S(5)	2.701(3)	Sb(2)−S(13)#1	2.722(4)
Sb(2)−S(4)	2.728(3)	Sb(2)−S(4)	2.735(3)
Sb(2)−S(13)#1	2.782(3)	Sb(2)−S(5)	2.760(4)
Sb(3)−S(4)	2.419(3)	Sb(3)−S(4)	2.408(3)
Sb(3)−S(6)	2.507(3)	Sb(3)−S(6)	2.505(3)
Sb(3)−S(7)	2.519(3)	Sb(3)−S(7)	2.518(4)
Sb(4)−S(7)	2.486(3)	Sb(4)−S(7)	2.488(3)
Sb(4)−S(16)#2	2.501(3)	Sb(4)−S(16)#2	2.501(4)
Sb(4)−S(5)	2.526(3)	Sb(4)−S(5)	2.504(3)
Sb(5)−S(9)	2.399(3)	Sb(5)−S(9)	2.403(3)
Sb(5)−S(6)	2.508(3)	Sb(5)−S(6)	2.506(4)
Sb(5)−S(8)	2.615(3)	Sb(5)−S(8)	2.604(3)
Sb(5)−S(7)	2.926(3)	Sb(5)−S(7)	2.911(3)
Sb(6)−S(8)	2.449(3)	Sb(6)−S(8)	2.449(3)
Sb(6)−S(10)	2.515(3)	Sb(6)−S(10)	2.511(4)
Sb(6)−S(13)	2.682(3)	Sb(6)−S(13)	2.745(3)
Sb(6)−S(9)	2.835(3)	Sb(6)−S(9)	2.749(4)
Sb(7)−S(10)	2.425(3)	Sb(7)−S(10)	2.424(3)
Sb(7)−S(11)	2.475(3)	Sb(7)−S(11)	2.478(3)
Sb(7)−S(12)#3	2.503(3)	Sb(7)−S(12)#3	2.502(4)
Sb(8)−S(13)	2.446(3)	Sb(8)−S(13)	2.436(3)
Sb(8)−S(12)	2.490(3)	Sb(8)−S(11)	2.487(4)
Sb(8)−S(11)	2.500(3)	Sb(8)−S(12)	2.489(3)
Sb(9)−S(14)	2.470(3)	Sb(9)−S(14)	2.469(3)
Sb(9)−S(3)	2.472(3)	Sb(9)−S(3)	2.477(3)
Sb(9)−S(5)	2.695(3)	Sb(9)−S(5)	2.651(4)
Sb(9)−S(15)	2.789(3)	Sb(9)−S(15)	2.830(4)
Sb(10)−S(15)	2.418(3)	Sb(10)−S(15)	2.413(3)
Sb(10)−S(16)	2.467(3)	Sb(10)−S(16)	2.464(3)
Sb(10)−S(14)	2.530(3)	Sb(10)−S(14)	2.515(4)

Compound **1**: Symmetry transformations: #1: *x*–1, *y*, *z*+1; #2: *x*+1/2, –*y*+1, *z*–1/2; #3: *x*–1/2, –*y*+2, *z*+1/2;

Compound **2**: Symmetry transformations: #1: *x*–1, *y*, *z*+1; #2: *x*+1/2, –*y*+1, *z*–1/2; #3: *x*, *y*, *z*–1;

Table 2. Selected Bond Angles (°) for 1 and 2

1		**2**	
Angle	(°)	Angle	(°)
S(2)−Sb(1)−S(3)	97.22(11)	S(2)−Sb(1)−S(3)	97.35(11)
S(2)−Sb(1)−S(1)	87.77(10)	S(2)−Sb(1)−S(1)	87.60(11)
S(3)−Sb(1)−S(1)	100.85(11)	S(3)−Sb(1)−S(1)	100.56(11)
S(1)−Sb(2)−S(2)	85.56(10)	S(1)−Sb(2)−S(2)	85.88(11)
S(1)−Sb(2)−S(5)	89.19(10)	S(1)−Sb(2)−S(13)#1	90.60(11)
S(2)−Sb(2)−S(5)	90.73(10)	S(2)−Sb(2)−S(13)#1	94.60(11)
S(1)−Sb(2)−S(4)	85.66(10)	S(1)−Sb(2)−S(4)	85.63(10)
S(2)−Sb(2)−S(4)	170.79(10)	S(2)−Sb(2)−S(4)	171.47(10)
S(5)−Sb(2)−S(4)	91.96(10)	S(13)#1−Sb(2)−S(4)	84.64(10)
S(1)−Sb(2)−S(13)#1	89.62(10)	S(1)−Sb(2)−S(5)	87.61(11)
S(2)−Sb(2)−S(13)#1	93.61(10)	S(2)−Sb(2)−S(5)	89.58(11)
S(5)−Sb(2)−S(13)#1	175.40(10)	S(13)#1−Sb(2)−S(5)	175.32(10)
S(4)−Sb(2)−S(13)#1	83.52(9)	S(4)−Sb(2)−S(5)	90.91(10)
S(4)−Sb(3)−S(6)	98.81(11)	S(4)−Sb(3)−S(6)	97.93(11)
S(4)−Sb(3)−S(7)	91.00(10)	S(4)−Sb(3)−S(7)	91.35(11)
S(6)−Sb(3)−S(7)	95.03(10)	S(6)−Sb(3)−S(7)	95.20(11)
S(7)−Sb(4)−S(16)#2	88.21(11)	S(7)−Sb(4)−S(16)#2	88.21(11)
S(7)−Sb(4)−S(5)	94.13(11)	S(7)−Sb(4)−S(5)	94.72(11)
S(16)#2−Sb(4)−S(5)	88.94(10)	S(16)#2−Sb(4)−S(5)	89.55(11)
S(9)−Sb(5)−S(6)	95.99(11)	S(9)−Sb(5)−S(6)	94.61(12)

To be continued

S(9)−Sb(5)−S(8)	89.43(11)	S(9)−Sb(5)−S(8)	88.93(11)
S(6)−Sb(5)−S(8)	93.01(10)	S(6)−Sb(5)−S(8)	93.31(11)
S(9)−Sb(5)−S(7)	85.12(10)	S(9)−Sb(5)−S(7)	85.20(10)
S(6)−Sb(5)−S(7)	85.65(10)	S(6)−Sb(5)−S(7)	86.09(10)
S(8)−Sb(5)−S(7)	174.22(10)	S(8)−Sb(5)−S(7)	174.03(10)
S(8)−Sb(6)−S(10)	93.16(11)	S(8)−Sb(6)−S(10)	92.60(11)
S(8)−Sb(6)−S(13)	87.15(10)	S(8)−Sb(6)−S(13)	85.46(10)
S(10)−Sb(6)−S(13)	91.30(10)	S(10)−Sb(6)−S(13)	91.22(11)
S(8)−Sb(6)−S(9)	83.50(10)	S(8)−Sb(6)−S(9)	84.73(11)
S(10)−Sb(6)−S(9)	101.03(10)	S(10)−Sb(6)−S(9)	100.84(12)
S(13)−Sb(6)−S(9)	164.89(10)	S(13)−Sb(6)−S(9)	164.77(11)
S(10)−Sb(7)−S(11)	96.12(11)	S(10)−Sb(7)−S(11)	97.40(11)
S(10)−Sb(7)−S(12)#3	92.47(11)	S(10)−Sb(7)−S(12)#4	91.23(11)
S(11)−Sb(7)−S(12)#3	85.35(10)	S(11)−Sb(7)−S(12)#4	85.54(11)
S(13)−Sb(8)−S(12)	101.01(11)	S(13)−Sb(8)−S(12)	101.25(11)
S(13)−Sb(8)−S(11)	93.88(10)	S(13)−Sb(8)−S(11)	93.45(11)
S(12)−Sb(8)−S(11)	92.85(10)	S(11)−Sb(8)−S(12)	91.92(12)
S(14)−Sb(9)−S(3)	99.00(11)	S(14)−Sb(9)−S(3)	99.00(11)
S(14)−Sb(9)−S(5)	78.65(10)	S(14)−Sb(9)−S(5)	79.77(11)
S(3)−Sb(9)−S(5)	95.54(10)	S(3)−Sb(9)−S(5)	95.17(11)
S(14)−Sb(9)−S(15)	81.43(10)	S(14)−Sb(9)−S(15)	81.02(11)
S(3)−Sb(9)−S(15)	84.52(10)	S(3)−Sb(9)−S(15)	84.12(11)
S(5)−Sb(9)−S(15)	159.85(10)	S(5)−Sb(9)−S(15)	160.45(10)
S(15)−Sb(10)−S(16)	98.96(11)	S(15)−Sb(10)−S(16)	98.78(11)
S(15)−Sb(10)−S(14)	88.03(11)	S(15)−Sb(10)−S(14)	88.94(11)
S(16)−Sb(10)−S(14)	89.38(10)	S(16)−Sb(10)−S(14)	89.21(11)
Sb(2)−S(1)−Sb(1)	94.46(11)	Sb(2)−S(1)−Sb(1)	94.26(11)
Sb(1)−S(2)−Sb(2)	91.50(10)	Sb(1)−S(2)−Sb(2)	91.75(10)
Sb(9)−S(3)−Sb(1)	115.85(13)	Sb(9)−S(3)−Sb(1)	115.72(15)
Sb(3)−S(4)−Sb(2)	103.30(11)	Sb(3)−S(4)−Sb(2)	102.78(12)
Sb(4)−S(5)−Sb(9)	104.35(11)	Sb(4)−S(5)−Sb(9)	103.85(12)
Sb(4)−S(5)−Sb(2)	93.37(10)	Sb(4)−S(5)−Sb(2)	93.19(11)
Sb(9)−S(5)−Sb(2)	119.57(12)	Sb(9)−S(5)−Sb(2)	120.18(11)
Sb(3)−S(6)−Sb(5)	94.49(11)	Sb(3)−S(6)−Sb(5)	94.01(12)
Sb(4)−S(7)−Sb(3)	99.12(11)	Sb(4)−S(7)−Sb(3)	98.91(12)
Sb(4)−S(7)−Sb(5)	97.12(10)	Sb(4)−S(7)−Sb(5)	97.83(11)
Sb(3)−S(7)−Sb(5)	84.76(9)	Sb(3)−S(7)−Sb(5)	84.59(10)
Sb(6)−S(8)−Sb(5)	95.63(10)	Sb(6)−S(8)−Sb(5)	94.34(10)
Sb(5)−S(9)−Sb(6)	91.26(11)	Sb(5)−S(9)−Sb(6)	91.78(11)
Sb(7)−S(10)−Sb(6)	102.86(11)	Sb(7)−S(10)−Sb(6)	103.11(13)
Sb(7)−S(11)−Sb(8)	102.22(11)	Sb(7)−S(11)−Sb(8)	102.06(13)
Sb(8)−S(12)−Sb(7)#4	119.14(12)	Sb(8)−S(12)−Sb(7)#6	95.11(10)
Sb(8)−S(13)−Sb(6)	101.86(12)	Sb(9)−S(14)−Sb(10)	102.96(13)
Sb(8)−S(13)−Sb(2)#5	103.52(11)	Sb(8)−S(13)−Sb(6)	101.92(11)
Sb(6)−S(13)−Sb(2)#5	95.11(10)	Sb(2)#7−S(13)−Sb(6)	94.93(11)
Sb(9)−S(14)−Sb(10)	96.81(11)	Sb(9)−S(14)−Sb(10)	97.15(11)
Sb(10)−S(15)−Sb(9)	91.50(10)	Sb(10)−S(15)−Sb(9)	90.57(11)
Sb(10)−S(16)−Sb(4)#6	101.89(11)	Sb(10)−S(16)−Sb(4)#8	101.88(13)

Compound **1**: Symmetry transformations: #1: *x*–1, *y*, *z*+1; #2: *x*+1/2, –*y*+1, *z*–1/2; #3: *x*–1/2, –*y*+2, *z*+1/2;
#4: *x*+1/2, –*y*+2, *z*–1/2; #5: *x*+1, *y*, *z*–1; #6: *x*–1/2, –*y*+1, *z*+1/2.

Compound **2**: Symmetry transformations: #1: *x*–1, *y*, *z*+1; #2: *x*+1/2, –*y*+1, *z*–1/2;
#4: *x*–1/2, –*y*+2, *z*+1/2; #6: *x*+1/2, –*y*+2, *z*–1/2; #7: *x*+1, *y*, *z*–1; *x*–1/2, #8: *x*–1/2, –*y*+1, *z*+1/2;

Table 3. Selected Hydrogen Bond Lengths (Å) and Bond Angles (°) for 1 and 2

1				
D−H···A	d(D−H)	d(H···A)	d(D···A)	∠DHA
N(1)−H(1A)···S(2)	0.89	2.65	3.471(10)	154
N(1)−H(1B)···S(14)#6	0.89	2.55	3.406(10)	163
N(1)−H(1C)···S(14)	0.89	2.48	3.335(10)	162
N(1)−H(1C)···S(16)	0.89	2.89	3.331(10)	112
N(1)−H(1D)···S(3)#7	0.89	2.70	3.367(10)	132
N(1)−H(1D)···S(15)#7	0.89	2.79	3.390(10)	126
N(2)−H(2A)···S(10)#3	0.89	2.78	3.475(10)	136
N(2)−H(2A)···S(11)#3	0.89	2.64	3.366(11)	139
N(2)−H(2B)···S(11)#8	0.89	2.65	3.300(10)	131
N(2)−H(2C)···S(10)	0.89	2.47	3.220(10)	142
N(2)−H(2D)···S(4)	0.89	2.39	3.198(10)	151
2				
D−H···A	d(D−H)	d(H···A)	d(D···A)	∠DHA
N(1)−H(1A)···S(2)	0.88	2.73	3.549(5)	154
N(1)−H(1B)···S(14)#8	0.88	2.53	3.382(5)	162
N(1)−H(1C)···S(14)	0.88	2.45	3.305(5)	162
N(1)−H(1C)···S(16)	0.88	2.84	3.270(6)	112
N(1)−H(1D)···S(3)#10	0.89	2.66	3.321(5)	133
N(1)−H(1D)···S(15)#10	0.89	2.76	3.340(5)	125
N(2)−H(2A)···S(10)#4	0.89	2.74	3.433(5)	136
N(2)−H(2A)···S(11)#4	0.89	2.61	3.306(4)	137
N(2)−H(2B)···S(11)#9	0.88	2.57	3.231(4)	132
N(2)−H(2C)···S(6)	0.88	2.74	3.170(5)	111
N(2)−H(2C)···S(10)	0.88	3.12	3.939(4)	142
N(2)−H(2D)···S(4)	0.88	2.31	3.121(5)	153

Compound **1**: Symmetry transformations: #3: *x*–1/2, –*y*+2, *z*+1/2; #6: *x*–1/2, –*y*+1, *z*+1/2; #7: *x*+1/2, –*y*+1, *z*+1/2; #8: *x*, *y*, *z*+1. Compound **2**: Symmetry transformations: #4: *x*–1/2, –*y*+2, *z*+1/2; #8: *x*–1/2, –*y*+1, *z*+1/2; #9: *x*, *y*, *z*+1; #10: *x*+1/2, –*y*+1, *z*+1/2

2. 4 Acid-base resistance experiment

30 mg sample (**1** or **2**) was placed in a 20 mL glass bottle with 15 mL acidic (pH = 0) and alkaline (pH = 12) solution, respectively, which was stirred vigorously for 10 h. Then the mixture was separated into solid and liquid, and the separated solid products were washed with water and ethanol.

2. 5 Electrochemical experiment

5 mg sample (**1** or **2**) was placed in a sample tube with 0.2 mL water, which was sequentially added by 40 uL anhydrous ethanol and 10 uL naphthol. The mixture was sonicated and shaken in an ultrasonic system for 8 h. Then 50 uL of the mixture was deposited on a 1 × 4 cm^2 conductive glass with a sample deposition area of 1 × 1 cm^2, which was used as a photoanode. Finally, electrochemical experiments were performed in a three-electrode system via an electrochemical workstation using 0.5 M sodium sulfate salt solution as the electrolyte.

3 RESULTS AND DISCUSSION

3. 1 Discussion on synthesis and crystal structures

1 and **2** were synthesized by the solvothermal method. **1** could be easily obtained by mixing 0.5 mmol $Sb(Ac)_3$ and 1.5 mmol S in the mixed solvents of 3 mL NH_3H_2O and 0.5 mL $N_2H_4H_2O$, while **2** was afforded by a similar reaction except that the additional reagent KCl (1.6 mmol) was added, and the amount of solvents was adjusted to 2 mL NH_3H_2O with 1 mL $N_2H_4H_2O$. In the synthesis of **2**, if KCl was replaced with K_2CO_3 or the amount of S exceeded 1.5 mmol, the by-production $(NH_4)_2Sb_4S_7$ would be generated. Therefore, KCl plays an important role in the synthesis of **2**. In addition, the crystals of **1** and **2** could not be obtained without $N_2H_4H_2O$. Therefore, the presence of $N_2H_4H_2O$ in the reaction processes was necessary.

SCXRD analyses show that **1** and **2** crystallize in monoclinic space group *Pn*. Their asymmetric units both contain ten unique Sb sites and sixteen S sites, but two $[NH_4]^+$ in **1** and 1.4 K^+ and 0.6 $[NH_4]^+$ in **2** (Fig. 1a). Since the two compounds are isomorphic, only the structure of **1** was analyzed in detail. As shown in Figs. 1b and 1c, the anionic

layer of $[Sb_{10}S_{16}]^{2-}$ consists of three different coordination modes of Sb(III), namely $[SbS_3]$ (for Sb(1), Sb(3), Sb(4), Sb(7), Sb(8) and Sb(10)), $[SbS_4]$ (for Sb(5), Sb(6) and Sb(9)), and $[SbS_5]$ (for Sb(2)). Then the $Sb(9)S_4$ and $Sb(10)S_3$ units are jointed together via corner-sharing to form a binuclear $[Sb_2S_5]$ cluster. $Sb(3)S_3$ and $Sb(5)S_4$ or $Sb(5)S_4$ and $Sb(6)S_3$ units also form the binuclear $[Sb_2S_5]$ cluster. $Sb(9)S_4$, $Sb(1)S_3$ and $Sb(2)S_5$ units are connected together via corner-sharing to form a trinuclear $[Sb_3S_7]$ cluster; $Sb(6)S_4$, $Sb(7)S_3$ and $Sb(8)S_3$ units are jointed together via corner-sharing to get a trinuclear $[Sb_3S_7]$ cluster; $Sb(2)S_5$, $Sb(3)S_3$ and $Sb(4)S_3$ units are linked together by corner-sharing to give a trinuclear $[Sb_3S_8]$ cluster. Then, three $[Sb_2S_5]$, two $[Sb_3S_8]$ and one $[Sb_3S_7]$ units are assembled by corner-sharing into a waved $[Sb_{10}S_{16}]_n^{2n-}$ anionic layer (Fig. 1c). As shown in Tables 1 and 2, the Sb−S bond lengths scatter over a range from 2.399 to 2.926 Å and corresponding S−Sb−S angles are in the range of 78.65 ～ 175.40°. Their bond lengths and angles are comparable to those of reported polymeric anions $[Sb_5S_8]^{2-}$ or $[Sb_{10}S_{16}]^{2-}$ in the literature[11, 18, 38-40]. Additionally, the NH_4^+ cations are located at the interlayer space of anionic layers, which interact with two adjacent $[Sb_{10}S_{16}]_n^{2n-}$ layers through N−H··· S bonds, resulting in a three-dimensional supramolecular network (Figs. 1d, 2e and 2f). From Fig. 1 and Table 3, N−H··· S hydrogen bonds are found in the range of 3.198(10) ～ 3.475(10) Å, and N−H··· S angles vary from 112.3° to 163.0° in **1** (Table 3).

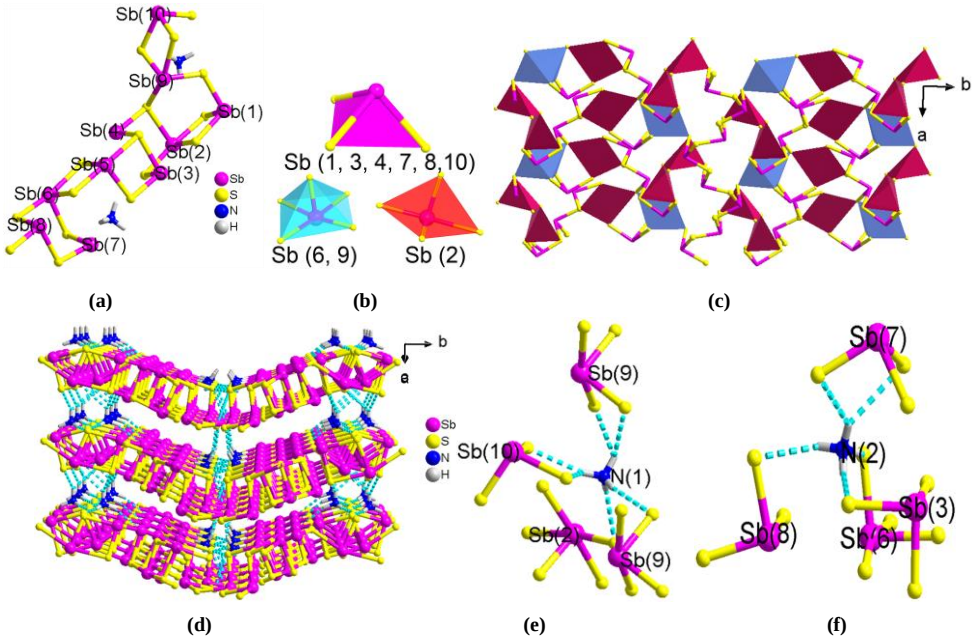

Fig. 1. (a) Asymmetric unit of $(NH_4)_2Sb_{10}S_{16}$; (b) Coordination modes of $[SbS_3]$, $[SbS_4]$ and $[SbS_5]$ in $[Sb_{10}S_{16}]$; (c) 2*D* anionic layer of $[Sb_{10}S_{16}]_n^{2n-}$ viewed along the *c*-axis (The red and blue polyhedra represent $[SbS_4]$ and $[SbS_5]$, respectively); (d) a three-dimensional supramolecular network formed by N−H ··S bonds between NH_4^+ cations and $[Sb_{10}S_{16}]_n^{2n-}$ anionic layer; the N−H ··S bonds of N(1)−H ··S (e) and N(2)−H ··S (f)

The anionic $[Sb_{10}S_{16}]_n^{2n-}$ layers of **1** and **2** resemble that of ASb_5S_8 (A = K, Tl)[11] with the same space group of *Pn*. The $[Sb_{10}S_{16}]_n^{2n-}$ anionic layers have also been found in $[C_6H_{17}N_3]Sb_{10}S_{16}$[18], $(C_3H_{12}N_2)[Sb_{10}S_{16}]$[38], $[H_3N(CH_2)_3NH_3]Sb_{10}S_{16}$[39] and $[C_6H_{18}N_2]Sb_{10}S_{16}H_2O$[40] (Table 4). However, these compounds present distinct cell parameters and crystallize in three types of space groups, that is, type I: *Pn* for compounds **1**, **2** and ASb_5S_8 (A = K, Tl); type II: $P2_1/c$ for $[C_6H_{17}N_3]Sb_{10}S_{16}$ and $[C_6H_{18}N_2]Sb_{10}S_{16}H_2O$; type III: $P2_1/n$ for $(C_3H_{12}N_2)[Sb_{10}S_{16}]$ and $[H_3N(CH_2)_3NH_3]Sb_{10}S_{16}$. If considering the additional secondary Sb−S interactions in interlayers, the above $[Sb_{10}S_{16}]_n^{2n-}$ layers can be defined as 3*D* structures. As shown in Fig. 2, the type I $[Sb_{10}S_{16}]_n^{2n-}$ layer features unique units of six $[SbS_3]$, three $[SbS_4]$ and one $[SbS_5]$ (Fig. 2a); type II $[Sb_{10}S_{16}]_n^{2n-}$ layer includes unique units of nine $[SbS_3]$ and one $[SbS_4]$ (Fig. 2b); type III $[Sb_{10}S_{16}]_n^{2n-}$ layer contains $[SbS_3]$ units only (Fig. 2c). Fig. 2 clearly shows the difference of tortuosity of anionic layer in the three types of $[Sb_{10}S_{16}]_n^{2n-}$ layers.

Table 4. Comparison of Crystal Parameters of 1 with Other Thioantimonates with the Sb:S Ratio of 1:1.6

	1	KSb_5S_8	$[C_6H_{17}N_3]Sb_{10}S_{16}$	$[C_6H_{18}N_2]Sb_{10}S_{16}\cdot H_2O$	$(C_3H_{12}N_2)Sb_{10}S_{16}$	$[H_3N(CH_2)_3NH_3]Sb_{10}S_{16}$
S.G.	*Pn*	*Pn*	$P2_1/c$	$P2_1/c$	$P2_1/n$	$P2_1/n$
a/Å	8.128	8.137	11.530	11.537	17.480	18.359(4)
b/Å	19.459	19.501	25.042	25.110	10.922	10.927(2)
c/Å	9.103	9.062	13.709	13.748	18.030	17.389(3)
β/°	91.73	91.93	111.25	111.286	111.42	111.44(2)
V/Å^3	1439.1	1437.2	3689.1	3711.0	3204.6	3247.1

S.G. = space group; $[C_6H_{17}N_3]^{2+}$ = doubly-protonated 2-piperazine-N-ethylamine; $[C_6H_{18}N_2]^{2+}$ = doubly-protonated 1,2-diaminopropane; $[C_3H_{12}N_2]^{2+}$ = doubly-protonated *N*,*N*-diethylethylenediamine; $[H_3N(CH_2)_3NH_3]^{2+}$ = doubly-protonated 1,3-propanediamine

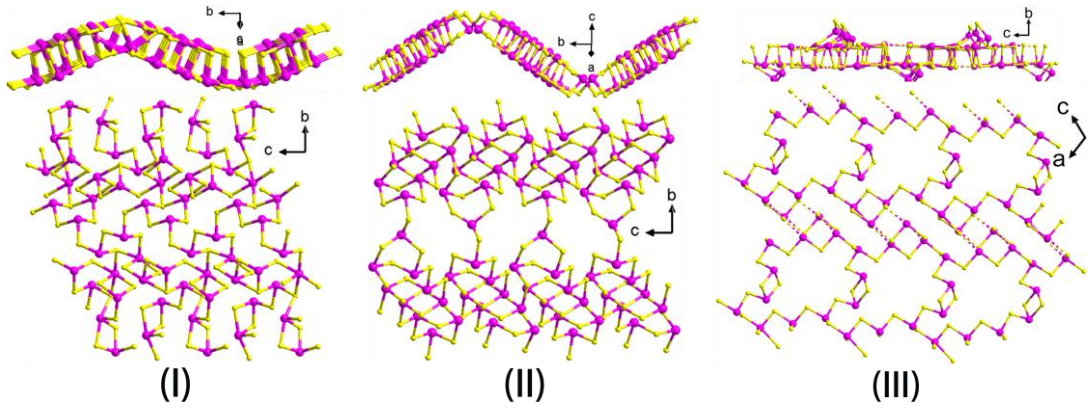

(a) (b) (c)

Fig. 2. Comparison of anionic layers for 1 (a), $[C_6H_{17}N_3]Sb_{10}S_{16}$ (b) and $(C_3H_{12}N_2)Sb_{10}S_{16}$ (c)

3. 2 Powder X-ray diffraction patterns, TG and UV-vis spectra

As shown in Fig. 3a, PXRD patterns for **1** and **2** match well with their corresponding simulated ones, indicating the phase-purity. In addition, the two compounds were added to acidic (pH = 0) and alkaline (pH = 12) solutions in order to investigate their acid-base resistances. **1** and **2** are stable even under acidic or basic solutions by comparing the PXRD patterns of pristine compounds and soaking products (Fig. 3b). The results confirm that the 2*D* anionic layer of $[Sb_{10}S_{16}]_n^{2n-}$ can be maintained under strong acidic and alkaline conditions, thus indicating good acid and base resistances for both compounds.

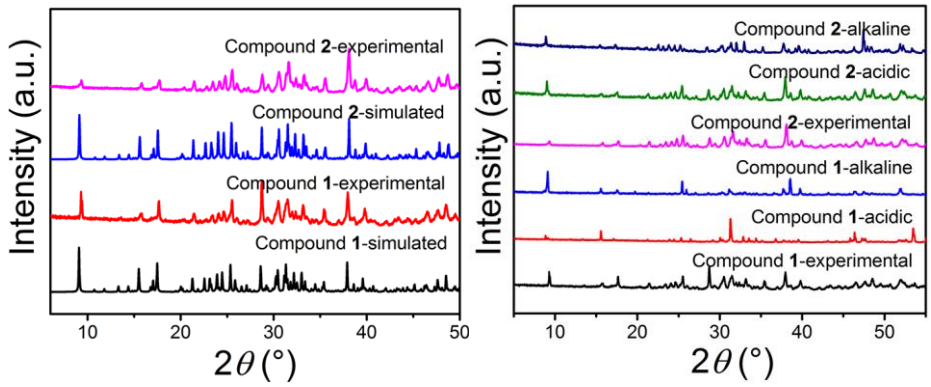

(a) (b)

Fig. 3. (a) Simulated and experimental PXRD patterns of 1 and 2; (b) PXRD patterns of the pristine 1 and 2 and their corresponding products soaked in the acidic or alkaline solutions for 10 h

The thermal stabilities of **1** and **2** were studied by TGA in a N_2 atmosphere from 30 to 800 ℃. TG curves are shown in Fig. 5a. They show the weight loss of 4.05% from 30 to 325 ℃ for **1** (the theoretical value of 3.96%) and 1.18% from 30 to 330 ℃ for **2** (the theoretical value of 1.17%), corresponding to the escape of NH_3 and H_2S molecules, respectively. The optical

absorption edges of **1** and **2** are 1.82 and 1.79 eV, respectively, falling in the range for semiconductor materials (Fig. 5b). Apparently, the lower optical absorption edge of **1** than that of **2** is consistent with its darker color than that of **2** (Fig. 5b).

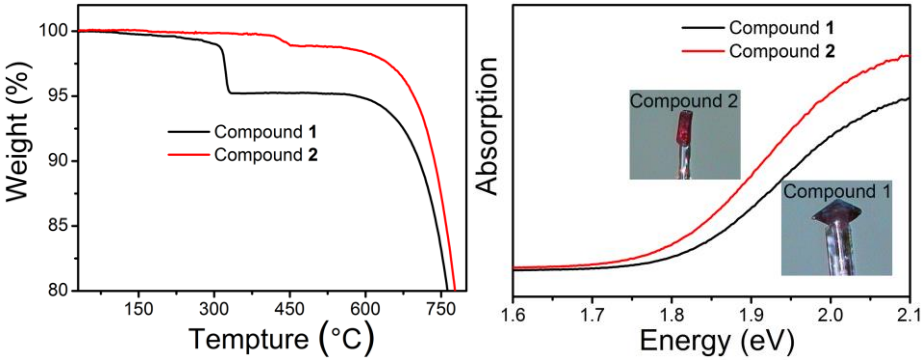

(a) **(b)**

Fig. 4. TG curve (a) and optical absorption spectra (b) of compounds 1 and 2. Insert image: photograph of a single-crystal for compounds 1 and 2

3. 3 Photoelectric properties

The photoelectric properties of **1** and **2** were investigated by measuring their photocurrent responses under visible light irradiation ($\lambda \geqslant 420$ nm) using a standard three-electrode system. From Fig. 5, the rapid and consistent photocurrent responses of **1** and **2** were performed in a multiple 10 sec switching period under visible light irradiation. **2** exhibits a stronger transient photocurrent response, which is about twice that of **1.** It can be confirmed that **2** has higher photogenerated electron transfer efficiency and photogenerated electron-hole pairs separation efficiency than **1** under visible light irradiation[44]. Meanwhile, the repeatable anodic photocurrent responses indicate that **1** and **2** belong to *n*-type (electron-conducting) semiconductor[45, 46].

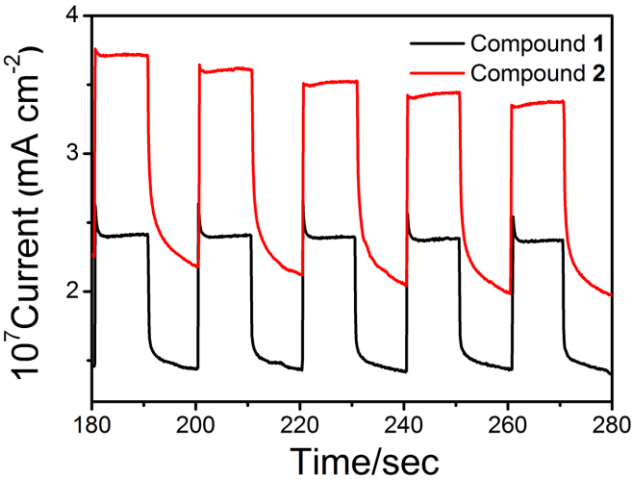

Fig. 5. Photocurrent responses of 1 and 2 under visible light irradiation ($\lambda \geqslant 420$ nm)

4 CONCLUSION

In conclusion, two new thioantimonates(III) were synthesized by a simple solvothermal method, and their structures, stabilities and optoelectronic properties were studied. They have the same anionic layer of $[Sb_{10}S_{16}]_n^{2n-}$. The acquisition of **2** could be simply achieved by adding KCl during the preparation of **1**. The stability experiments indicate that **1** and **2** have excellent thermal stability and acid-based resistances. The photoelectric results and optical absorption spectra confirm that **1** and **2** are semiconductors and **2** shows better photoelectric property than **1**. The current compounds enrich the structural diversity of thioantimonates(III), especially thioantimonates(III) with NH_4^+ cations. The synthetic route described in this work should be an effective way to prepare novel thioantimonates.

REFERENCES

(1) Zheng, N.; Bu, X. H.; Vu, H.; Feng, P. Y. Open-framework chalcogenides as visible-light photocatalysts for hydrogen generation from water.*Angew. Chem. Int. Ed.* **2005**, 44, 5299−5303.

(2) Yu, J. M.; Cai, T.; Ma, Z. J.; Wang, F.; Wang, H.; Yu, J. P.; Xiao, L. L.; Cheng, F. F.; Xiong, W. W. Using thiol-amine solvent mixture to prepare main group heterometallic chalcogenides.*Inorg. Chim. Acta* **2020**, 509, 119698−7.

(3) Feng, M. L.; Kong, D. N.; Xie, Z. L.; Huang, X. Y. Three-dimensional chiral microporous germanium antimonysulfide with ion-exchange properties. A*ngew. Chem. Int. Ed.* **2008**, 47, 8623−8626.

(4) Ding, N.; Kanatzidis, M. G. Selective incarceration of caesium ions by Venus flytrap action of a flexible framework sulfide.*Nat. Chem.* **2010**, 2, 187−191.

(5) Chung, I.; Kanatzidis, M. G. Metal chalcogenides: a rich source of nonlinear optical materials.*Chem. Mater.* **2014**, 26, 849−869.

(6) Bag, S.; Trikalitis, P. N.; Chupas, P. J.; Armatas, G. S.; Kanatzidis, M. G. Porous semiconducting gels and aerogels from chalcogenide clusters. *Science* **2007**, 317, 490−493.

(7) Zheng, N. F.; Bu, X. G.; Wang, B.; Feng, P. Y. Microporous and photoluminescent chalcogenide zeolite analogs. *Science* **2002**, 298, 2366−2369.

(8) Xiong, W. W.; Miao, J. W.; Ye, K. Q.; Wang, Y.; Liu, B.; Zhang, Q. C. Threading chalcogenide layers with polymer chains*Angew. Chem. Int. Ed.* **2015**, 54, 546−550.

(9) Wang, F.; Yang, D. D.; Liao, Y. Y.; Ma, Z. J.; Hu, B.; Wang, Y. Q.; Xiong, W. W.; Huang, X. Y. Synthesizing crystalline chalcogenidoarsenates in thiol-amine solvent mixtures. *Inorg. Chem.* **2020**, 59, 2337−2347.

(10) Parise, J. B. An antimony sulfide with a two-dimensional, intersecting system of channels. *Science* **1991**, 251, 293−294.

(11) Berlepsch, P.; Miletich, R.; Armbruster, T. The crystal structures of synthetic KSb_5S_8 and $(Tl_{0.598}, K_{0.402})Sb_5S_8$ and their relation to parapierrotite ($TlSb_5S_8$). *Z. Kristallogr.* **1999**, 214, 57−63.

(12) Zhou, J.; Dai, J.; Bian, G. Q.; Li, C. Y. Solvothermal synthesis of group 13～15 chalcogenidometalates with chelating organic amines. *Coord. Chem. Rev.* **2009**, 253, 1221−1247.

(13) Sheldrick, W. S.; Wachhold, M. Chalcogenidometalates of the heavier group 14 and 15 elements. *Coord. Chem. Rev.* **1998**, 176, 211−322.

(14) Kiebach, R.; Nather, C.; Bensch, W. Solvothermal synthesis of $(C_6H_{17}N_3)Sb_{10}S_{16}$: a new thioantimonate(III) with an *in-situ* formed organic amine cation. *Z. Naturforsch., B: Chem. Sci.* **2004**, 59, 1314−1319.

(15) Vaqueiro, P.; Darlow, D. P.; Powell, A. V.; Chippindale, A. M. Solvothermal synthesis of novel antimony sulphides containing $[Sb_4S_7]^{2-}$ units. *Solid State Ionics* **2004**, 172, 601−605.

(16) Spetzler, V.; Nather, C.; Bensch, W. $(C_6N_2H_{18})Sb_4S_7$ a thioantimonate(III) with a layered $[Sb_4S_7]^{2-}$ anion in the presence of a diprotonated amine as structure director. *Z. Naturforsch., B: Chem. Sci.* **2006**, 61, 715−720.

(17) Ko, Y. H.; Tan, K. M.; Parise, J. B.; Darovsky, A. Synthesis of a novel two-dimensional antimony sulfide, $[C_4H_{10}N]_2Sb_8S_{13}·0.15H_2O$, and its structure solution using synchrotron imaging plate data. *Chem. Mater.* **1996**, 8, 493−496.

(18) Wang, X. Q.; Liebau, F. Synthesis and structure of $(CH_3NH_3)_2Sb_8S_{13}$: a nanoporous thioantimonate(III) with a 2-dimensional channel system. *J. Solid State Chem.* **1994**, 111, 385−389.

(19) Spetzler, V.; Kiebach, R.; Nather, C.; Bensch, W. Two novel thioantimonates(III) with the same stoichiometric Sb:S ratio but different crystal structures: solvothermal synthesis, crystal structures, thermal stability and spectroscopy of $(C_6N_3H_{17})Sb_6S_{10}$ and $(C_7N_2H_{13})_3Sb_9S_{15}$. *Z. Anorg. Allg. Chem.* **2004**, 630, 2398−2404.

(20) Sheldrick, W. S.; Hausler, H. J. On the preparation and crystal-structure of $Cs_3Sb_5S_9$, $Cs_3Sb_5Se_9$. *Z. Anorg. Allg. Chem.* **1988**, 561, 149−156.

(21) Zhu, A. M.; Jia, D. X.; Wang, P.; Zhang, Y. Solvothermal synthesis and crystal structure of a layered thioantimonate(III) $[C_4H_9NH_3]_2Sb_4S_7$. *Chin. J. Struc. Chem.* **2007**, 26, 1298−1302.

(22) Mertz, J. L.; Fard, Z. H.; Malliakas, C. D.; Manos, M. J.; Kanatzidis, M. G. Selective removal of Cs^+, Sr^{2+}, and Ni^{2+} by $K_{2x}Mg_xSn_{3-x}S_6$ (x = 0.5～1) (KMS-2) relevant to nuclear waste remediation. *Chem. Mater.* **2013**, 25, 2116−2127.

(23) Manos, M. J.; Kanatzidis, M. G. Highly efficient and rapid Cs^+ uptake by the layered metal sulfide $K_{2x}Mn_xSn_{3-x}S_6$ (KMS-1). *J. Am. Chem. Soc.* **2009**, 131, 6599−6607.

(24) Zhang, X.; Yi, N.; Hoffmann, R.; Zheng, C.; Lin, J.; Huang, F. Semiconductive $K_2MSbS_3(SH)$ (M = Zn, Cd) featuring one-dimensional $^1_\infty[M_2Sb_2S_6(SH_2)]^{4-}$ chains. *Inorg. Chem.* **2016**, 55, 9742−9747.

(25) Wang, K. Y.; Liu, H. W.; Zhang, S.; Ding, D.; Cheng, L.; Wang, C. Selenidostannates and a silver selenidostannate synthesized in deep eutectic

solvents: crystal structures and thermochromic study. *Inorg. Chem.* **2019**, 58, 2942−2953.

(26) Wang, K. Y.; Ding, D.; Zhang, S.; Wang, Y.; Liu, W.; Wang, S.; Wang, S. H.; Liu, D.; Wang, C. Preparation of thermochromic selenidostannates in deep eutectic solvents. *Chem. Commun.* **2018**, 54, 4806−4809.

(27) Cai, T.; Zhu, J. N.; Cheng, F. F.; Li, P.; Li, W.; Zhao, M. Y.; Xiong, W. W. Growing crystalline selenidostannates in deep eutectic solvent. *Inorg. Chim. Acta* **2019**, 484, 214−218.

(28) Ma, Z. M.; Weng, F.; Wang, Q. R.; Tang, Q.; Zhang, G. H.; Zheng, C.; Han, R. P. S.; Huang, F. Q. Low temperature synthesis and structures of alkaline earth metal chalcogenides $Ba_3Cu_4SbS_6OH$, $BaCuSbS_3$ and $BaCu_2S_2$. *RSC Adv.* **2014**, 4, 28937−28940.

(29) Sheldrick, W. S.; Wachhold, M. Solventothermal synthesis of solid-state chalcogenidometalates. *Angew. Chem. Int. Ed.* **1997**, 36, 207−224.

(30) Du, K. Z.; Feng, M. L.; Li, L. H.; Hu, B.; Ma, Z. J.; Wang, P.; Li, J. R.; Wang, Y. L.; Zou, G. D.; Huang, X. Y. $[Ni(phen)_3]_2Sb_{18}S_{29}$: a novel three-dimensional framework thioantimonate(III) templated by $[Ni(phen)_3]$ complexes. *Inorg. Chem.* **2012**, 51, 3926−3928.

(31) Yang, D. D.; Li, W.; Xiong, W. W.; Li, J. R.; Huang, X. Y. Ionothermal synthesis of discrete supertetrahedral T*n* (*n* = 4, 5) clusters with tunable components, band gaps, and fluorescence properties. *Dalton Trans.* **2018**, 47, 5977−5984.

(32) Cordier, G.; Schwidetzky, C.; Schafer, H. New SbS_2 strings in the $BaSb_2S_4$ structure. *J. Solid State Chem.* **1984**, 54, 84−88.

(33) Cordier, G.; Schafer, H.; Schwidetzky, C. The crystal-structure of $SrSb_4S_7 \cdot 6H_2O$. *Z. Naturforsch., B: Chem. Sci.* **1984**, 39, 131−134.

(34) Graf, H. A.; Schafer, H. Preparation and crystal-structure of $K_2Sb_4S_7$. *Z. Naturforsch. B Chem. Sci.* **1972**, B27, 735−739.

(35) Kiebach, R.; Nather, C.; Sebastian, C. P.; Mosel, B. D.; Pottgen, R.; Bensch, W. $[C_6H_{21}N_4][Sb_9S_{14}O]$: solvothermal synthesis, crystal structure and characterization of the first non-centrosymmetric open Sb-S-O framework containing the new $[SbS_2O]$ building unit. *J. Solid State Chem.* **2006**, 179, 3082−3086.

(36) Powell, A. V.; Boissiere, S.; Chippindale, A. M. $[(NH_3CH_2CH_2CH_2NH_2CH_2)_2]_{0.5}Sb_7S_{11}$: a new two-dimensional antimony sulfide with antimony-antimony bonding. *Chem. Mater.* **2000**, 12, 182−187.

(37) Dittmar, G.; Schafer, H. Preparation and crystal-structure of $Cs_2Sb_4S_7$. *Z. Anorg. Allg. Chem.* **1978**, 441, 98−102.

(38) Puls, A.; Nather, C.; Bensch, W. 2-Ammoniopropylammonium dodeca-mu-sulfido-tetrasulfidodecaantimony. *Acta Crystallogr., Sect. E: Crystallogr. Commun.* **2006**, 62, M674−M676.

(39) Wang, X. Q. Synthesis and crystal-structure of a new microporous thioantimonate(III) $[H_3N(CH_2)_3NH_3]Sb_{10}S_{16}$. *Eur. J. Solid State Inorg. Chem.* **1995**, 32, 303−312.

(40) Zhang, M.; Sheng, T. L.; Huang, X. H.; Fu, R. B.; Wang, X.; Hu, S. M.; Xiang, S. C.; Wu, X. T. Solvothermal synthesis, crystal structure, and thermal stability of three-layered thioantimonate(III) complexes: $[Ni(C_3H_{10}N_2)_3]Sb_4S_7$, $[C_4H_{14}N_2]Sb_8S_{13}H_2O$, and $[C_6H_{18}N_2]Sb_{10}S_{16}H_2O$. *Eur. J. Inorg. Chem.* **2007**, 1606−1612.

(41) Dittmar, G.; Schafer, H. Preparation and crystal-structure of $(NH_4)_2Sb_4S_7$. *Z. Anorg. Allg. Chem.* **1977**, 437, 183−187.

(42) Volk, K.; Bickert, P.; Kolmer, R.; Schafer, H. Preparation and crystal-structure of NH_4SbS_2. *Z. Naturforsch., B: Chem. Sci.* **1979**, 34, 380−382.

(43) Sheldrick, G. M. Crystal structure refinement with SHELXL. *Acta Crystallogr., Sect. C: Cryst. Struct. Commun.* **2015**, 71, 3−8.

(44) Luo, Q. P.; Yu, X. Y.; Lei, B. X.; Chen, H. Y.; Kuang, D. B.; Su, C. Y. Reduced graphene oxide-hierarchical ZnO hollow sphere composites with enhanced photocurrent and photocatalytic activity. *J. Phys. Chem. C* **2012**, 116, 8111−8117.

(45) Li, G.; Miao, J. W.; Cao, J.; Zhu, J.; Liu, B.; Zhang, Q. C. Preparation and photoelectrochemical behavior of 1,4,6,8,11,13-hexazapentacene (HAP). *Chem. Commun.* **2014**, 50, 7656−7658.

(46) Zhang, Q. C.; Liu, Y.; Bu, X. H.; Wu, T.; Feng, P. Y. A rare (3,4)-connected chalcogenide superlattice and its photoelectric effect. *Angew. Chem. Int. Ed.* **2008**, 47, 113−116.